

# UC Riverside

## UC Riverside Previously Published Works

### Title

Surface-bound sacrificial electron donors in promoting photocatalytic reduction on titania nanocrystals

### Permalink

<https://escholarship.org/uc/item/62x1261h>

### Journal

Nanoscale, 11(41)

### ISSN

2040-3364

### Authors

Feng, Ji  
Yang, Fan  
Ye, Yifan  
[et al.](#)

### Publication Date

2019-11-07

### DOI

10.1039/c9nr05453g

Peer reviewed

# Surface-Bound Sacrificial Electron Donors in Promoting Photocatalytic Reduction on Titania Nanocrystals†

Ji Feng,<sup>a</sup> Fan Yang,<sup>a</sup> Yifan Ye,<sup>b</sup> Wenshou Wang,<sup>c</sup> Xiayi Yao,<sup>d</sup> Qingsong Fan,<sup>a</sup> Luntao Liu,<sup>c</sup> Rashed M. Aleisa,<sup>a</sup> Jinghua Guo<sup>b</sup> and Yadong Yin<sup>a\*</sup>

Titania nanocrystals have been investigated for fast color switching through photocatalytic reduction of dyes and hexacyanometalate pigments. Here we reveal that direct binding of sacrificial electron donors (SEDs) to the surface of the titania nanocrystals can significantly promote charge transfer rate by more efficiently scavenging photogenerated holes and release more photogenerated electrons for the reduction reactions. Using diethylene glycol (DEG) as an example, we show that its binding to the nanoparticle surface, which can be achieved either during or after the nanoparticle formation, greatly enhances the photocatalytic reduction in comparison to the case where free DEG molecules are simply added as external SEDs.

## Introduction

Titania has received continued attention as a promising photocatalyst due to its excellent photocatalytic performance, good stability, high abundance, and low toxicity.<sup>1-5</sup> Upon light excitation, the photo-generated electrons and holes play different roles in the photocatalytic process.<sup>6</sup> For example, the photo-generated electrons can reduce electron acceptors, and the holes can oxidize electron donors.<sup>6</sup> While the oxidation capability of the photo-generated holes has been widely investigated for degradation of organic pollutants, cancer treatment, and antibacterial applications,<sup>7-11</sup> the photo-generated electrons have been explored as efficient reducing agents in addressing many environment and energy-related issues.<sup>12-14</sup> In particular, recently, titania nanocrystals have been employed as a vital component in constructing photochromic organic-inorganic hybrid color switching systems, which can change color reversibly in response to light stimulation. In a typical system, titania nanocrystals were synthesized in diethylene glycol (DEG) with Pluronic copolymer and used as photocatalysts for a quick reduction of methylene blue (MB) to *leuco* methylene blue (LMB).<sup>15</sup> The photocatalytic reduction of MB and oxidation of LMB in air was reversible, resulting in the switching of color between colorless and blue, which had been applied for an ink-free light printable rewritable paper.<sup>16</sup> To meet the demands of rewritable paper application, the efficiency of the photocatalysts should be optimized. Therefore, understanding the mechanism of the photocatalysis on titania is of great importance for the design and optimization of the color switching system.

The efficiency of the photocatalytic process by titania itself depends strongly on its phase, surface area, particle size, and crystallinity.<sup>13</sup> After the photo-excitation, the photo-generated electrons and holes migrate to the surface of titania to be trapped by the surface  $\text{-Ti}^{\text{IV}}\text{-OH}$  groups.<sup>17, 18</sup> Meanwhile, the charge carriers also recombine in bulk or on the surface of titania and undermine their reactivity.

Only the surviving charge carriers can participate in photocatalytic redox reactions. Unfortunately, the recombination rate of charge carriers is in the same order of magnitude with their trapping rate and much higher than the interfacial charge transfer rate.<sup>18</sup> Therefore, prohibiting the recombination of charge carriers plays a significant role in optimization the photocatalytic efficiency of titania. In addition, because the charge transfer between an electron and an electron acceptor ( $\sim$ ms) is much slower than that between a hole and an electron donor (100 ns), improving the efficiency of photocatalytic reduction reactions still remains a challenge.

Sacrificial electron donors (SEDs), such as methanol, ethanol, oxalic acid, formaldehyde, etc., are often employed as additives in photocatalytic reactions to scavenge the photo-generated holes and suppress the recombination of charge carriers.<sup>19-21</sup> As a result, photo-generated electrons are released, and the photocatalytic reduction rate of the reactants are accelerated.<sup>22</sup> However, the reduction rate is still limited because the additives are free in suspension. The hole-scavenging efficiency depends on the adsorption of the additives to the surface of the nanoparticles, which is affected by the concentration of the additives and nanoparticles and their interactions.

Efficient scavenging of photo-generated holes was observed experimentally in titania with chemisorbed polyhydroxy molecules.<sup>23</sup> Time-resolved transient absorption spectroscopy showed the fast hole-scavenging rate of carbohydrates and C2-C6 polyols in the titania colloidal solutions. It was suggested that free holes could be directly trapped by the surface bonded polyols. It was also found by calculation that dissociatively adsorbed glucose and ethylene glycol on the (101) surface of anatase titania were more efficient than the molecularly adsorbed ones towards hole-scavenging.<sup>24</sup> Despite this, the polyols were just simply mixed with titania nanocrystals during the photocatalysis as additives.<sup>25-27</sup> The physical adsorption of the polyols on titania nanocrystals limited the photocatalytic performance of such materials.

<sup>a</sup> Department of Chemistry, University of California, Riverside, CA 92521, USA  
E-mail: yadong.yin@ucr.edu

<sup>b</sup> Advanced Light Source, Lawrence Berkeley National Laboratory, Berkeley, CA 94720, USA

<sup>c</sup> National Engineering Research Center for Colloidal Materials, School of Chemistry and Chemical Engineering, Shandong University Ji'Nan 250100, P.R. China

<sup>d</sup> School of Chemistry and Materials Engineering, Changshu Institute of Technology, Changshu 215500, P. R. China

†Electronic Supplementary Information (ESI) available: [details of any supplementary information available should be included here]. See DOI: 10.1039/x0xx00000x

In this paper, we aim to highlight the importance of binding SEDs to the photocatalyst surface in promoting photocatalytic reduction reactions. By using DEG as an example, we show that its binding to the surface of titania nanocrystals can dramatically enhance the photocatalytic reduction of redox dyes comparing with the case with freeform DEG in the solution. The surface-bound DEG is introduced to the titania nanocrystals by hydrolysis and condensation of a titanium glycolate precursor, which is a stable metal complex formed by coordination between Ti ions and the hydroxyl groups of DEG.<sup>28, 29</sup> Although titanium glycolates have been widely used as structure directing agents for the shape-controlled synthesis of titania particles, the products often need to be treated at a high temperature for crystallization, which eliminates the surface polyols in the end.<sup>30, 31</sup> Investigation of titania synthesized from titanium glycolate towards photocatalytic reduction reactions, although very important, remains blank. In our present work, direct hydrolysis and condensation of the titanium glycolate precursors in a controllable manner lead to the formation of titania nanocrystals with high crystallinity and a large amount of surface-bound SEDs. The structure and surface properties of titania nanocrystals were analyzed to confirm the anatase phase of the nanocrystals, the non-existence of oxygen vacancies, and the presence of Ti-O-C bonds. The surface-bound DEG is sufficient to support many cycles of photocatalytic reduction of redox dyes, making the hybrid titania nanoparticles excellent active components for applications that require photo-induced reduction but do not allow the presence of free SED molecules.

## Experimental

### Chemicals

Titanium (IV) chloride ( $\text{TiCl}_4$ ), diethylene glycol (DEG), tetraethyl orthosilicate (TEOS), titanium (IV) butoxide (TBOT), hydroxypropyl cellulose (HPC,  $M_w \sim 80,000$ ) and methylene blue (MB) were purchased from Sigma-Aldrich. Ammonia (28-30 wt. %) and acetonitrile (ACN) were purchased from Fisher Chemical. All Chemicals were analytical grade and used as received without further purification. Solutions were prepared with deionized (DI) water ( $18.2 \text{ M}\Omega/\text{cm}$ ) produced from the Milli-Q system (Millipore).

### Synthesis of $\text{TiO}_2$ nanocrystals

$\text{TiO}_2$  nanocrystals were synthesized by hot injection of 0.2 mL  $\text{TiCl}_4$  into 20 ml diethylene glycol (DEG). A small amount of  $\text{H}_2\text{O}$  (0.2 mL) was employed for the hydrolysis of  $\text{TiCl}_4$ . The mixture was heated at 220 °C for 3 hours to crystallize  $\text{TiO}_2$ . The product was washed several times with acetone to remove excess DEGs then redispersed in water.

### Synthesis of $\text{SiO}_2@ \text{TiO}_2$ nanospheres

$\text{SiO}_2$  nanospheres were synthesized by mixing TEOS (0.86 mL) with DI water (4 mL), ethanol (23 mL) and ammonia (0.75 mL). After stirring for 4 h at room temperature, silica nanoparticles were separated from the solvents by centrifugation and washed 3 times with ethanol, then re-dispersed in a mixture of hydroxypropyl cellulose (HPC, 50 mg), ethanol (20 mL), ACN (7 mL) and ammonia (200  $\mu\text{L}$ ). Titania coating was done by quickly injecting a mixture of TBOT (1 mL), ACN (1 mL) and ethanol (3 mL) into the  $\text{SiO}_2$

dispersion. After stirring for 2 hours,  $\text{SiO}_2@ \text{TiO}_2$  nanospheres were collected using centrifugation, washed with ethanol and water, and dried at 60 °C.

### Surface modification of $\text{SiO}_2@ \text{TiO}_2$ nanospheres

The as-made  $\text{SiO}_2@ \text{TiO}_2$  nanospheres were calcined at 700 °C to crystallize  $\text{TiO}_2$ . Surface modification was done by heating the  $\text{SiO}_2@ \text{TiO}_2$  nanospheres in DEG at 220 °C for 2 hours. After washing with water to remove the excess amount of DEG, the nanospheres, named as ST-700-DEG, were dried at room temperature.

### Photocatalytic reduction of MB

In a typical photocatalytic reduction, the concentration of photocatalysts and MB are 0.2 mg/mL and  $8.2 \times 10^{-6} \text{ M}$ , respectively. UV irradiation was performed under a UV torch (5 W). UV-vis spectra are measured directly without isolation of the photocatalysts.

### Characterizations

The morphology of the nanostructures was investigated using a Philips Tecnai T12 transmission electron microscope (TEM) at an accelerating voltage of 120 kV. The samples for TEM observation were supported on a copper grid with a carbon micro-grid. Powder X-ray diffraction (XRD) patterns were recorded on a PANalytical Empyrean diffractometer with  $\text{Cu K}\alpha$  radiation  $\lambda = 1.5406 \text{ \AA}$  with a graphite monochromator (40 kV, 40 mA). The Fourier transform infrared spectroscopy (FT-IR) spectra were acquired on a Nicolet 6700 FTIR spectrometer. X-ray photoelectron spectroscopy (XPS) characterization was carried out on a Kratos AXIS ULTRADLD XPS system equipped with an Al  $\text{K}\alpha$  monochromated X-ray source and a 165-mm mean radius electron energy hemispherical analyzer. XAS data were measured on BL 8.0.1.4 at the Advanced Light Source, Lawrence Berkeley National Laboratory. Total electron yield (TEY) signal was collected by monitoring the sample drain current. Powder samples were pressed on an indium foil to make a thin film under ambient air and then transferred to the vacuum chamber for the O K-edge XAS measurements. Standard anatase  $\text{TiO}_2$  film was applied as reference and energy calibration purpose. The energy resolution of XAS was set to be 0.1 eV. TGA was done on a Netzsch TG 209 F1 Libra in an air flow of 50 mL/min, from room temperature to 800 °C. The heating rate was 20 °C/min.

## Results and discussion

Wavelength, nm

Wavelength, nm

Time, s

**Figure 1.** (a-c) Large-scale TEM image (a), high-resolution TEM image (b), and XRD pattern (c) of titania nanocrystals synthesized in DEG; (d) UV-vis spectra of the photocatalytic reduction of MB on titania nanocrystals upon 365 nm UV irradiation; (e) UV-vis spectra of the re-coloration of MB in dark under ambient conditions; (f) Averaged photocatalytic reduction of MB over titania nanocrystals of 5 runs.

The hot injection of  $\text{TiCl}_4$  into DEG leads to the formation of a transparent glycolate precursor, which remains stable in air at room temperature over months. It can be hydrolyzed upon the addition of water and then condensed into titania nanocrystals at elevated temperature. In a typical process, after heating at 220 °C for 3 hours, the solution became turbid, and titania nanocrystals of ~5-10 nm with irregular shapes were obtained, as shown in Figure 1a. The nanocrystals were washed with acetone and water for 5 times to remove the excess amount of DEG, and re-dispersed in water. The interplanar spacing of titania nanocrystals in the HRTEM image was measured to be 0.352 nm, which corresponds to the (101) lattice plane of the anatase phase (Figure 1b). The crystalline structure of the titania nanocrystals was characterized by XRD analysis (Figure 1c), with all diffraction peaks being indexed to the anatase phase (JCPDS card no. 21-1272). The domain size of the products was calculated according to the Sherrer formula:  $\tau = (k\lambda)/(\beta\cos\theta)$ , where  $\tau$  is the average crystalline domain size,  $k$  is the shape factor with a typical value of 0.9,  $\lambda$  is the X-ray wavelength (0.1548 nm),  $\beta$  is the line broadening full width at half maximum (FWHM) peak height of the (101) peak, and  $\theta$  is the Bragg angle. The average domain size was found to be approximately 4.0 nm, which is in good agreement with the TEM observation.

The as-synthesized titania nanocrystals were found to be active for the photocatalytic reduction of MB. Upon UV irradiation under UV (365 nm, 5 W), an aqueous mixture containing titania nanocrystals (0.2 mg/ml) and MB ( $8.2 \times 10^{-6}$  M) displayed a color change from blue to colorless, suggesting the reduction of MB to LMB.<sup>15</sup> After the removal of UV light, LMB can be oxidized back to MB by dissolved oxygen, leading to a color recovery to blue. To precisely monitor the reduction of MB over UV irradiation, UV-vis spectra of the system

were measured directly without the removal of titania nanocrystals from the system. Figure 1d shows the absorption of the solution upon UV irradiation, measured every 5 seconds. The peak at about 662 nm, which was attributed to the absorption of MB, decreased gradually with the increase of the UV irradiation time. After 30 s, MB was fully bleached. The recovery of MB is shown in Figure 1e. When the system was kept in the dark, complete oxidation of LMB to MB could be achieved in 6 hours. To better evaluate the photocatalytic performance of the titania nanocrystals, the photocatalytic reduction of MB was repeated for another 4 times (Figure S1), and the averaged absorbance change by time was plotted and shown in Figure 1f. For all of the trials, the complete reduction of MB could be achieved in 30 seconds. The physical properties of titania nanocrystals after 1 run of the photocatalytic reduction were characterized. As shown in Figure S3, the crystal sizes, phase and surface functionality remained unchanged after the photocatalysis, suggesting that the titania nanocrystals were stable during the photocatalysis. The cycling performance of titania nanocrystals for the reduction of MB has also been tested. As shown in Figure S2, MB could be fully bleached for 5 cycles.

The amount of DEG was determined by TGA analysis. Figure S4 shows a two-step pattern for weight loss in the temperature range of 30 to 250 and 250 to 600 °C. The first weight loss is due to the desorption of physically adsorbed water, DEG and its derivatives, and the second one could be attributed to the pyrolysis of DEG. The amount of DEG on titania surface was 15 % of the total weight. The presence of surface-bound DEG on titania nanocrystals was confirmed by FTIR. Figure 2a shows the FTIR spectra of pure DEG and the titania nanocrystals. The absorption peaks at 892, 1051, 1122 and 1230  $\text{cm}^{-1}$  correspond to the  $-\text{OC}_2\text{H}_4$  stretching, C-O

stretching C-C-O and C-O-C stretching in pure DEG, respectively. The absorption peaks at around 1352, 1456, 2872, and 2900  $\text{cm}^{-1}$  are due to the vibration of  $\text{CH}_2$  in DEG. These peaks are well maintained in the FTIR spectrum of titania nanocrystals, indicating the presence of DEG moieties on the surface of titania. It is worth noting that the absorption peak of C-O at 1051  $\text{cm}^{-1}$  in the spectrum of DEG shifts to 1080  $\text{cm}^{-1}$  in the spectrum of titania nanocrystals, which suggests the formation of C-O-Ti.<sup>32</sup>

In our previous study, we found that oxygen vacancies could also serve as effective SEDs to scavenge the photogenerated holes.<sup>33</sup> In the current case, the existence of oxygen vacancies in titania nanocrystals was ruled out by XAS studies. The O K-edge XAS represents the transition from O 1s to O 2p, which is sensitive to the electronic and chemical environment of the investigated samples.<sup>34</sup> As shown in Figure 2b, the reference anatase  $\text{TiO}_2$  O K-edge spectrum shows four peaks, with two sharp ones at energy region of 528 to 537 eV and two broad ones at 537 to 550 eV, representing the O 2p final states hybridized with Ti 3d and Ti 4sp, respectively. The XAS signal of titania nanocrystals also showed similar spectrum profiles compared to the reference anatase  $\text{TiO}_2$ , showing two sharp O 2p-Ti 3d peaks and two broad O 2p-Ti 4sp peaks. The obvious peak broadening of the features compared to the reference anatase  $\text{TiO}_2$  suggested reduced crystal sizes of the titania nanocrystals and the influence of the DEG functional groups.<sup>35</sup> The energy difference of the first two sub-peaks represents the crystal field splitting strength. The well-resolved two sub-peaks of O 2p-Ti 3d hybridization state of titania nanocrystals, as well as almost the same crystal field splitting strength of the titania nanocrystals and the reference anatase  $\text{TiO}_2$  indicate the well-maintained chemical structure of the titania nanocrystals, suggesting the absence of the oxygen vacancies.<sup>36</sup>

Elemental composition and bonding of DEG on the surface of titania nanocrystals were further characterized by XPS, shown in Figure 2c-f. All the peaks were calibrated by taking the binding energy of adventitious carbon at 284.8 eV as a reference. The survey spectrum (Figure 2c) of titania nanocrystals shows that the nanocrystals only contain C, O, and Ti. XPS in the C 1s region (Figure 2d) shows three components at 284.8, 285.6 and 286.4 eV, which can be assigned to C-H, C-O-Ti, and C-O species, respectively.<sup>37</sup> The Ti-O-C bond is also confirmed by the peak at 530.5 eV in the O 1s region (Figure 2e). The peaks at 529.5, 531.5 and 532.4 eV are attributed to  $\text{O}^{2-}$  anions, Ti-OH in  $\text{TiO}_2$ , and C-O species, respectively.<sup>38, 39</sup> The peaks at 458.2 and 464.2 eV shown in Ti 2p region (Figure 2f) indicates that  $\text{Ti}^{4+}$  is the dominant form of titanium in the titania nanocrystals.

To confirm the role of DEGs as surface-bonded SEDs, we checked the surface functionality of titania nanocrystals after different periods of UV irradiation. During the experiment, the concentration of titania nanocrystals was kept at 10 mg/mL, and a UV lamp of 365 nm with the power of 300 W was used as the light source. After being irradiated for a certain period, titania nanocrystals were isolated by adding acetone to the dispersion and dried under vacuum at room temperature. Surface properties of the dried particles were characterized by using FTIR. As shown in Figure 3a, the C-O-Ti absorption at 1080  $\text{cm}^{-1}$  decreased with the prolonged UV irradiation, indicating the dissociation of DEG moieties from titania nanocrystals. After UV irradiation for 5 hours, nearly all the

DEG moieties were depleted from the surface of titania nanocrystals. Meanwhile, the absorption band at  $\sim 3200 \text{ cm}^{-1}$  increased, indicating the formation of more Ti-OH. The titania nanocrystals after 5 hours of UV irradiation were tested for the photocatalytic reduction of MB. As shown in Figure 3b, the intensity of the absorption peak of MB at  $\sim 662 \text{ nm}$  remained after UV irradiation for even 60 seconds. We can conclude from these results that titania nanocrystals without surface-bound DEG moieties will not photo-induce the reduction of MB. In other words, DEGs can work as surface-bound SEDs in the photocatalysis to scavenge the photo-generated holes, releasing photo-generated electrons for the reduction reaction.

We further show that DEG bound to the titania surface through post-processing can also serve as effective SEDs to promote photocatalytic reduction. Here we used a  $\text{SiO}_2@\text{TiO}_2$  core-shell nanostructure as a model for illustration. The  $\text{SiO}_2$  nanospheres were used as substrates to control the domain size of titania nanocrystals, improve the convenience for sample collection, and provide large surface area for efficient coating of titania. An amorphous titania shell ( $\sim 23 \text{ nm}$ ) was deposited to the surface of silica nanospheres through a sol-gel method according to our previous report, and then calcined at 700  $^\circ\text{C}$  to enhance crystallinity, producing a sample named as ST-700 (Figure S5).<sup>40</sup> The titania shell was found to be composed of anatase phase (Figure S6) with a domain size of  $\sim 4.1 \text{ nm}$ , which is similar to that of the titania nanocrystals synthesized in DEG at 220  $^\circ\text{C}$ . Surface modification of ST-700 core-shell nanostructures was done by refluxing the nanospheres in DEG at 220  $^\circ\text{C}$  for 2 hours. After that, the nanostructures were washed with water to remove the excess amount of DEG, dried, and named as ST-700-DEG.

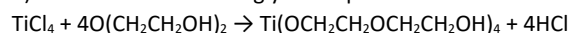
Surface modification of DEG moieties on ST-700 was confirmed by FTIR. Figure S7 shows the FTIR spectra of ST-700 before and after refluxing in DEG for 2 hours. The typical absorption peak at 1083  $\text{cm}^{-1}$  is attributed to the Si-O-Si vibration in both ST-700 and ST-700-DEG.<sup>41</sup> And a small shoulder at 951  $\text{cm}^{-1}$  of ST-700 is from the Si-O-Ti vibration.<sup>42</sup> After refluxing in DEG, three obvious absorption peaks at 1464, 1367 and 931  $\text{cm}^{-1}$  appeared, which corresponded to  $\text{CH}_2$  bending,  $\text{CH}_2$  wagging and CO stretching of DEG moieties, respectively, indicating the successful grafting of DEG moieties to the surface of ST-700. The existence of DEG moieties is also confirmed by the broadened absorption band at  $\sim 1080 \text{ cm}^{-1}$  that is due to the C-OH and C-O-Ti stretching.

To confirm that post-surface-bonded DEG can also serve as effective SEDs, here we compare the photocatalytic reduction rate of MB by using ST-700, ST-700 with physically mixed DEG and ST-700-DEG as catalysts. The concentrations of all the photocatalysts were kept at 0.2 mg/mL. And the concentration of MB was set to be  $4.1 \times 10^{-6} \text{ M}$ . Again, the absorption of MB was measured without removal of the photocatalysts to avoid oxidation during isolation of the nanoparticles. Figure 4a shows the photocatalysis of MB in an ST-700 aqueous solution. Before UV irradiation, the absorption peak of MB was observed at 584 nm, indicating the presence of MB dimers and trimers, which was caused by the strongly adsorption of MB on surface of ST-700 through electrostatic interaction.<sup>43</sup> After UV irradiation for 60 seconds, the absorption peak slightly blue shifted to 577 nm, indicating the formation of more MB trimers by time. The intensity of MB displayed almost no change, suggesting that ST-

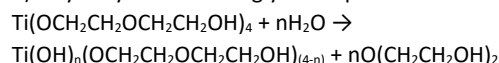
700 could not catalyze the reduction of MB in 60 seconds. Further, we found that the photocatalytic reduction of MB was not possible in a simple mixture of ST-700 and DEG. As shown in Figure 4b, the intensity of the absorption of MB did not change upon 60 seconds of UV irradiation. In contrast, the photocatalytic reduction of MB was fast in the presence of ST-700-DEG. As shown in Figure 4c, the intensity of the absorption of MB quickly decreased in the first 30 seconds. After keeping the suspension in the dark, the intensity recovered (dash line in Figure 4c), indicating the reversibility of color change. Comparing the photocatalytic performance of ST-700-DEG to ST-700 and the simple mixture of ST-700 and DEG, we can conclude that the titania with surface-bonded DEG is the most effective catalyst to promote the photocatalytic reduction.

Here, we propose the mechanism for the formation and photocatalysis of titania nanocrystals synthesized using DEG as both a solvent and a surface-bound SED. The reaction of  $\text{TiCl}_4$  with DEG produces a glycolate precursor which hydrolyzes and condenses at an elevated temperature by reacting with water. During the hydrolysis, the DEG moieties bonded with  $\text{Ti}^{4+}$  are replaced by the  $-\text{OH}$  groups from  $\text{H}_2\text{O}$ . The condensation of  $\text{Ti}-\text{OH}$  groups produces  $\text{Ti}-\text{O}-\text{Ti}$  structure and generates titania nanocrystals. As shown in Figure S8, the crystallinity of titania increases with prolonged heating time. The domain size was calculated to be 1.90, 2.45, and 3.97 nm for titania nanocrystals heated at 220 °C for 1, 2, and 3 hours, respectively. Because the insufficient amount of  $\text{H}_2\text{O}$  and the short time for hydrolysis, only part of the glycolate precursor can be converted to crystallized titania, leaving a large number of glycolate moieties on the nanocrystal surface. The formation mechanism can be concluded as below:

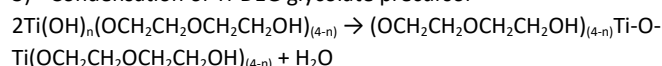
1) Formation of Ti-DEG glycolate precursor



2) Hydrolysis of Ti-DEG glycolate precursor



3) Condensation of Ti-DEG glycolate precursor



It is worth noting that the photocatalytic efficiency of titania nanocrystals is related to the crystallinity of titania and surface-

bonded DEG moieties, which are determined by the heating time. The heating time should be long enough to crystallize titania nanocrystals, but it should not be too long to deplete DEG moieties from the titania nanocrystals. We have compared the photocatalytic efficiency of titania nanocrystals synthesized after 3, 6, and 9 hours for the reduction of  $\text{Cr}(\text{VI})$ .<sup>44</sup> After heating for 9 hours, the photocatalytic performance decreased because of the substitution of DEG moieties by  $-\text{OH}$  groups.

The mechanism for the photocatalysis on titania nanocrystals is shown in Figure 5. Upon photo-excitation, the surface-bound DEG moieties will capture a hole, and form an alkoxy radical, which will then be oxidized to an aldehyde. The hopping of a trapped hole onto a carbon atom and the breakage of a C-H bond has been proposed by DFT simulation, which indicates the formation of a C=O double bond will lower the total energy of the material, which is favorable in the photocatalytic process.<sup>28</sup> Nucleophilic attack of water will take place for the recovery of the active site and release the oxidized SED.

## Conclusions

In summary, we highlight here the significant advantage of direct bonding of SEDs to the surface of titania nanocrystals in photocatalytic reduction reactions. Using DEG as a model SED, we show that its binding to titania nanocrystal surface either during nanocrystal formation or post-synthesis treatment can dramatically enhance the photocatalytic reduction in comparison to the case with a simple mixture of titania and DEG. When titania nanocrystals are synthesized directly from a glycolate precursor, it is important to control the heating to reach high crystallinity of the titania nanocrystals and at the same time to minimize the depletion of surface-bound SEDs. We believe understanding the importance of surface-bound SEDs can help the design of more efficient photocatalysts toward light-induced reduction reactions, which is of critical importance especially in the solid-state applications where high efficiency is desired, and the presence of free SED molecules is prohibitive, such as rewritable paper and smart materials.

## Conflicts of interest

There are no conflicts to declare.

## Acknowledgements

This work was jointly supported by UC Riverside and Korea Institute of Materials Science (Research Program (POC2930)) through the UC-KIMS Center for Innovation Materials for Energy and Environment. We also thank the U.S. National Science Foundation (DMR-0958796) for the support in XPS characterization. Acknowledgement is also made to the Central Facility for Advanced Microscopy and Microanalysis at UCR for help with TEM and XRD analysis.

**Keywords:** titania • photocatalytic reduction • surface-modification • sacrificial electron donor • nanocrystals

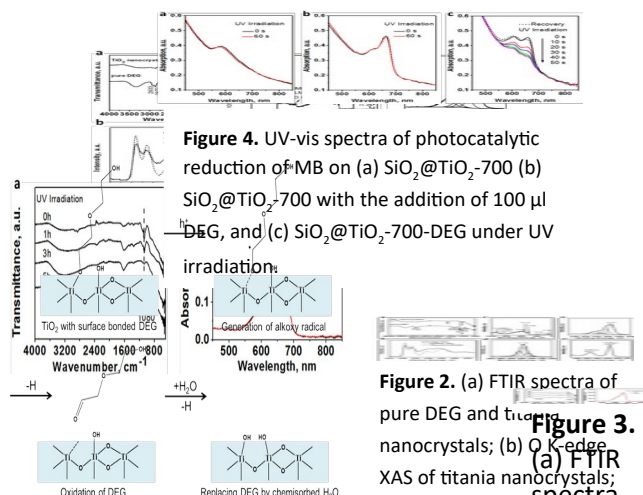


**Figure 5.** Schematic illustration of the change of titania surface upon UV irradiation.

**Figure 4.** UV-vis spectra of photocatalytic reduction of MB on (a)  $\text{SiO}_2@\text{TiO}_2$ -700 (b)  $\text{SiO}_2@\text{TiO}_2$ -700 with the addition of 100  $\mu\text{l}$  DEG, and (c)  $\text{SiO}_2@\text{TiO}_2$ -700-DEG under UV irradiation.

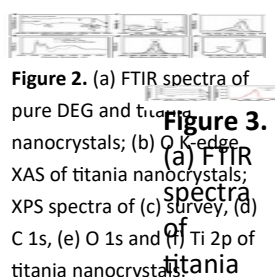


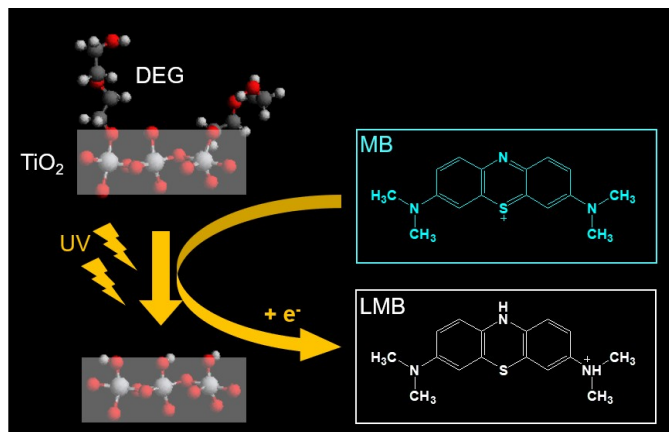
**Figure 2.** (a) FTIR spectra of pure DEG and titania nanocrystals; (b) O K-edge XAS of titania nanocrystals; XPS spectra of (c) survey, (d) C 1s, (e) O 1s and (f) Ti 2p of titania nanocrystals.

**Figure 3.** (a) FTIR spectra of titania nanocrystals upon UV irradiation.

## References

1. Y. K. Kho, A. Iwase, W. Y. Teoh, L. Mädler, A. Kudo and R. Amal, *J. Phys. Chem. C*, 2010, **114**, 2821.
2. A. A. Ismail and D. W. Bahnemann, *J. Mater. Chem.*, 2011, **21**, 11686.
3. A. Fujishima, X. Zhang and D. Tryk, *Surf. Sci. Rep.*, 2008, **63**, 515.
4. N. Nursam, X. Wang and R. Caruso, *ACS Comb. Sci.*, 2015, **17**, 548.
5. Y. K. Kho, A. Iwase, W. Y. Teoh, L. Madler, A. Kudo and R. Amal, *J Phys Chem C*, 2010, **114**, 2821.
6. A. L. Linsebigler, G. Lu and J. T. Yates, *Chem Mater.*, 1995, **95**, 735.
7. L. K. Adams, D. Y. Lyon and P. J. J. Alvarez, *Water Res.*, 2006, **40**, 3527.
8. J.-w. Seo, H. Chung, M.-y. Kim, J. Lee, I.-h. Choi and J. Cheon, *Small*, 2007, **3**, 850.
9. H. Liu, J. B. Joo, M. Dahl, L. Fu, Z. Zeng and Y. Yin, *Energy Environ. Sci.*, 2015, **8**, 286.
10. A. Fujishima, T. N. Rao and D. A. Tryk, *J. Photoch. Photobiol. C*, 2000, **1**, 1.
11. U. Gaya and A. Abdullah, *J. Photoch. Photobiol. C*, 2008, **9**, 1.
12. M. Huang, E. Tso, A. K. Datye, M. R. Prairie and B. M. Stange, *Environ. Sci. Technol.*, 1996, **30**, 3084.
13. D. Leung, X. Fu, C. Wang, M. Ni, M. Leung, X. Wang and X. Fu, *Chemosuschem*, 2010, **3**, 681.
14. A. Dhakshinamoorthy, S. Navalon, A. Corma and H. Garcia, *Energy Environ. Sci.*, 2012, **5**, 9217.
15. W. Wang, M. Ye, L. He and Y. Yin, *Nano Lett*, 2014, **14**, 1681.
16. W. Wang, N. Xie, L. He and Y. Yin, *Nat. Commun.*, 2014, **5**.
17. O. I. Micic, Y. Zhang, K. R. Cromack, A. D. Trifunac and M. C. Thurnauer, *J. Phys. Chem.*, 1993, **97**, 7277.
18. M. R. Hoffmann, S. T. Martin, W. Choi and D. W. Bahnemann, *Chem. Rev.*, 1995, **95**, 69.
19. W. Gao, R. Jin, J. Chen, X. Guan, H. Zeng, F. Zhang and N. Guan, *Catal. Today*, 2004, **90**, 331.
20. N. M. Dimitrijevic, I. A. Shkrob, D. J. Gosztola and T. Rajh, *J. Phys. Chem. C*, 2012, **116**, 878.
21. H. Xu, S. Ouyang, P. Li, T. Kako and J. Ye, *ACS Appl. Mater. Interfaces*, 2013, **5**, 1348.
22. M. Valari, A. Antoniadis, D. Mantzavinos and I. Poullos, *Catal. Today*, 2015, **252**, 190.
23. I. A. Shkrob, M. C. Sauer and D. Gosztola, *J. Phys. Chem. B*, 2004, **108**, 12512.
24. M.-H. Du, J. Feng and S. Zhang, *Phys. Rev. Lett.*, 2007, **98**, 066102.
25. K. E. Sanwald, T. F. Berto, W. Eisenreich, O. Y. Gutiérrez and J. A. Lercher, *J. Catal.*, 2016, **344**, 806.
26. J. Kennedy, H. Bahruji, M. Bowker, P. R. Davies, E. Bouleghimat and S. Issarapanacheewin, *Journal of Photochemistry and Photobiology A: Chemistry*, 2018, **356**, 451.
27. V. Kumaravel, M. D. Imam, A. Badreldin, R. K. Chava, J. Y. Do, M. Kang and A. Abdel-Wahab, *Catalysts*, 2019, **9**, 276.
28. V. W. Day, T. A. Eberspacher, M. H. Frey, W. G. Klemperer, S. Liang and D. A. Payne, *Chem. Mater.*, 1996, **8**, 330.
29. D. Wang, R. Yu, N. Kumada and N. Kinomura, *Chem. Mater.*, 1999, **11**, 2008.
30. Y. Wei, J. Zhu, Y. Gan and G. Cheng, *Advanced Powder Technology*, 2018, **29**, 2289.
31. H. Li, L. Zhang, J. K. Jo, C.-S. Ha, Y. A. Shchipunov and I. Kim, *J. Nanopart. Res.*, 2011, **13**, 2117.
32. N. Tangboriboon, A. M. Jamieson, A. Sirivat and S. Wongkasemjit, *Appl. Organomet. Chem.*, 2006, **20**, 886.
33. W. Wang, Y. Ye, J. Feng, M. Chi, J. Guo and Y. Yin, *Angew. Chem., Int. Ed.*, 2015, **54**, 1321.
34. Y. Ye, M. Kapilashrami, C.-H. Chuang, Y.-s. Liu, P.-A. Glans and J. Guo, *MRS Commun.*, 2017, **7**, 53.
35. L. Vayssieres, C. Persson and J.-H. Guo, *Appl. Phys. Lett.*, 2011, **99**, 183101.
36. W. Yan, Z. Sun, Z. Pan, Q. Liu, T. Yao, Z. Wu, C. Song, F. Zeng, Y. Xie, T. Hu and S. Wei, *Appl. Phys. Lett.*, 2009, **94**, 042508.
37. D. Sarkar, S. Ishchuk, D. H. Taffa, N. Kaynan, B. A. Berke, T. Bendikov and R. Yerushalmi, *J. Phys. Chem. C*, 2016, **120**, 3853.
38. X. Zou, G. Li, J. Zhao, J. Su, X. Wei, K. Wang, Y. Wang and J. Chen, *Int J Photoenergy*, 2012, DOI: 10.1155/2012/720183.
39. S. Umrao, S. Abraham, F. Theil, S. Pandey, V. Ciobota, P. K. Shukla, C. J. Rupp, S. Chakraborty, R. Ahuja, J. Popp, B. Dietzek and A. Srivastava, *RSC Adv.*, 2014, **4**, 59890.
40. J. B. Joo, Q. Zhang, I. Lee, M. Dahl, F. Zaera and Y. Yin, *Adv. Funct. Mater.*, 2012, **22**, 166.
41. C. Huang, H. Bai, Y. Huang, S. Liu, S. Yen and Y. Tseng, *Int J Photoenergy*, 2012, **2012**, 8.
42. N. Dhiman, B. P. Singh and A. K. Gathania, *J. Nanophotonics*, 2012, **6**, 063511.
43. B. Liu, L. Wen, K. Nakata, X. Zhao, S. Liu, T. Ochiai, T. Murakami and A. Fujishima, *Chem. Eur. J.*, 2012, **18**, 12705.
44. G. Chen, J. Feng, W. Wang, Y. Yin and H. Liu, *Water Res.*, 2017, **108**, 383.

ToC



Direct binding of sacrificial electron donors to the surface of titania nanocrystals significantly promotes photocatalytic reduction reactions.